



CHAPTER IV

RESULTS AND DISCUSSION

In this chapter, the results and discussion are divided into two main sections. First, catalyst characterization and catalytic testing are discussed in Sections 4.1, 4.2 and 4.3, respectively. The transformation of bioethanol to aromatic hydrocarbons was studied in this research work under the system of single catalytic bed and two consecutive beds. The catalysts and experimental design are summarized in Table 4.1. The Runs #1 to #4 entirely involve the aromatic production from bioethanol using single-bed catalytic system, which are carried out at 500 °C under atmospheric pressure. Especially, the Run #5, which is an additional test, is set up to investigate the ethylene production ability of the catalytic Bed #1 of two consecutive bed systems. Lastly, the Runs #6 to #9 relate to the investigation of bioethanol-based aromatic production using a dual-bed catalytic system. Ultimately, the best set of experimental results was employed as the basis in the economic pre-feasibility evaluation.

4.1 Characterization of Catalysts

This part discusses the characterization of catalysts by using several techniques to overview the difference on their characteristic and properties. BET was used to measure the physical properties of catalysts, including surface area and pore size.

Table 4.1 Catalysts and experimental design for the investigation of bioethanol-based aromatic production

# of run	Experimental Set	Catalyst on Bed #1 (@ 370 °C)	Catalyst on Bed #2 (@ 500 °C)	Abbreviation
<i>Single-bed catalytic systems</i>				
1	HZSM-5	-	HZSM-5	HZ5
2	2 %wt Ga ₂ O ₃ /HZSM-5	-	2 %wt Ga ₂ O ₃ /HZSM-5	GHZ5
3	2 %wt ZnO/HZSM-5	-	2 %wt ZnO/HZSM-5	ZHZ5
4	6.25 %wt ZnO-Al ₂ O ₃ + 93.75 %wt HZSM-5	-	6.25 %wt ZnO-Al ₂ O ₃ + 93.75 %wt HZSM-5	Z+HZ5
<i>Two consecutive-bed catalytic systems</i>				
5	0.5 %wt MgHPO ₄ /Al ₂ O ₃	0.5 %wt MgHPO ₄ /Al ₂ O ₃	-	EPC
6	0.5 %wt MgHPO ₄ /Al ₂ O ₃ :HZSM-5	0.5 %wt MgHPO ₄ /Al ₂ O ₃	HZSM-5	EPC:HZ5
7	0.5 %wt MgHPO ₄ /Al ₂ O ₃ :2 %wt Ga ₂ O ₃ /HZSM-5	0.5 %wt MgHPO ₄ /Al ₂ O ₃	2 %wt Ga ₂ O ₃ /HZSM-5	EPC:GHZ5
8	0.5 %wt MgHPO ₄ /Al ₂ O ₃ :2 %wt ZnO/HZSM-5	0.5 %wt MgHPO ₄ /Al ₂ O ₃	2 %wt ZnO/HZSM-5	EPC:ZHZ5
9	0.5 %wt MgHPO ₄ /Al ₂ O ₃ :6.25 %wt ZnO-Al ₂ O ₃ + 93.75 HZSM-5	0.5 %wt MgHPO ₄ /Al ₂ O ₃	6.25 %wt ZnO-Al ₂ O ₃ + 93.75 %wt HZSM-5	EPC:Z+HZ5

The surface area, pore volume, and pore diameter of the studied catalysts were measured by using BET technique, which are revealed in Table 4.2. The impregnation of gallium and zinc on the HZSM-5 zeolite results in the reduction of surface area and pore volume. Similarly, the surface area and pore volume of the mixed catalysts (zinc oxide alumina co-catalyst (ZnO-Al₂O₃) and HZSM-5) are also lower than those of HZSM-5. Nevertheless, the pore diameter of all modified catalysts is significantly higher. Possibly, gallium and zinc loading as well as physical mixing of ZnO-Al₂O₃ cause pore blocking, especially in a narrow pore. Thus, the average of pore diameter mostly contributed from macropores is slightly increased.

Table 4.2 Physical properties of HZSM-5 based catalysts

Catalyst	Surface area (m ² /g)	Pore volume (cm ³ /g)	Pore diameter (Å)
HZSM-5	549.7	0.189	5.843
Ga ₂ O ₃ /HZSM-5	415.0	0.152	6.675
ZnO/HZSM-5	461.3	0.153	6.061
ZnO-Al ₂ O ₃ + HZSM-5	419.5	0.154	6.850

4.2 Activity of Single-bed Catalytic Systems on Aromatic Production from Bioethanol

Since the investigation of catalyst efficiency in this work is mainly based on double-bed catalytic systems, each catalyst used in this work for bioethanol conversion to aromatic hydrocarbons needs to be proven first for its own activity.

For the single-bed catalytic systems, the catalyst testing was carried out at 500 °C under atmospheric pressure in every investigations. The liquid hour space velocity of 1.0 h⁻¹ was used. Three grams of a catalyst was packed in the second catalytic bed as described in Chapter 3. The reaction time was held for 5 hours for collecting the liquid product.

4.2.1 Effect of metal oxide loaded on HZSM-5

This section discusses about the influence of metal oxide loaded on the HZSM-5 zeolite catalysts. There are three catalysts investigated in this section; pure HZSM-5, gallium oxide, and zinc oxide supported on HZSM-5 catalyst. The effect of loading is discussed as follows.

The conversion of bioethanol obtained from both pure HZSM-5 and modified HZSM-5 is not significantly different according to the results shown in Table 4.3. For all catalyst testing, the obtained conversion is approximately in the range of 83 – 85 %. It can be seen that whether or not the HZSM-5 was modified by metal oxides, the bioethanol conversion is not significantly affected. In contrast, the metal oxide loading affects to the product distribution, which can be observed in Table 4.3, which the total gas and oil yields are specifically presented. The result reveals that approximately 56.2 % total gas yield and 10.3 % total oil yield are acquired from HZSM-5 without modification. In case of modified catalysts; that are, gallium oxide and zinc oxide-promoted HZSM-5, the yield of oil product is increased to 18.3 % and 13.2 %, which is improved around 78 % and 28 %, respectively. Additionally, the compositions of obtained oils mainly consist of aromatic hydrocarbons, especially mono-aromatic hydrocarbons. Besides the highest oil yield obtained from gallium oxide supported on the HZSM-5, it can be noticed that the highest aromatic yield are also obtained. When the total aromatics yields of all catalysts are compared, it is found that the dopants promoting the HZSM-5 catalyst can significantly improve the total aromatic yield. This is an evidence indicating that the modified catalysts can help to enhance the aromatic production from bioethanol.

For the gaseous product analysis, it is observed that the yield of gaseous product decreases in the order: HZ5 > ZHZ5 > GHZ5, which is in the opposite trend to the oil yield. In case of HZ5 and GHZ5, the gas compositions mainly consist of mixed C3 hydrocarbons followed by ethane. Moreover, the carbon dioxide is significantly produced in the case of modified HZSM-5 catalysts, in particular, the ZHZ5 catalyst.

Table 4.3 Product distribution over modified catalysts in the single-bed systems

	HZ5	GHZ5	ZHZ5
Ethanol Conversion (%)	85.0	83.4	82.8
Product yield (%)			
Total gas	56.2	48.5	53.7
Total oil	10.3	18.3	13.2
Total aromatics in oil	9.1	16.8	12.7
Gas Composition (%)			
Methane	10.1	10.9	8.9
Ethylene	7.6	6.4	5.8
Ethane	20.8	17.5	21.5
C3	40.9	36.6	12.5
C4	4.5	0.0	3.0
C5+	2.4	5.7	3.6
CO ₂	13.6	22.9	44.8
	100.0	100.0	100.0
Oil Composition (%)			
Monoaromatics	87	90.1	88.5
Diaromatics	1.3	1.7	7.9
Triaromatics	< 0.1	< 0.1	< 0.1
Non-aromatics	11.7	8.2	3.63
	100.0	100.0	100.0

Data were taken at the fifth hour of time-on-stream

$$Yield (\%) = \frac{\text{Total weight of any products (g)}}{\text{Total weight of converted bioethanol (g)}} \times 100$$

The enhancement of aromatic yield over modified HZSM-5 catalysts can be explained by the synergistic effect of bifunctional catalysts. The HZSM-5 zeolite alone is an acidic solid catalyst that is effective for cracking, dehydrogenation isomerization, and oligomerization to form heavier products, like aromatic hydrocarbons. However, the ability of aromatic formation over the HZSM-5 alone has limitations. Therefore, the addition of either suitable metals or metal oxides to HZSM-5 can help to improve some activity of the catalyst. Likewise, the reaction involving bioethanol conversion to aromatic hydrocarbons can be improved by Ga- or Zn-containing HZSM-5 catalyst, which can accelerate the aromatization by

improving dehydrogenation reaction (Brathos *et al.*, 2006). Generally, the catalysis of bioethanol dehydration to aromatic hydrocarbons over the modified HZSM-5 catalyst can be separated into two main steps. First, ethanol is initially activated on the acid side of HZSM-5 catalyst via dehydration reaction. Thus, the primary products are ethylene and water. Then, the ethylene can be further catalyzed by the acid site of HZSM-5 again through a carbenium ion mechanism to form carbenium ions. Subsequently, oligomerization is rapidly occurred, followed by isomerization, cyclization and/or cracking. For the case of gallium supported on the HZSM-5, the deposition of gallium species can improve the dehydrogenation activity of catalyst. Several intermediates (i.e. C1 and C3+) occurring during all previously mentioned reactions are more dehydrogenated. Then, the dehydrogenated products are possibly re-oligomerized, isomerized, cyclized, and aromatized on the acid sites of zeolite to form heavy products or aromatic hydrocarbons.

4.2.2 Effect of Hybrid Catalyst

In this part, ZnO-Al₂O₃ co-catalyst combined with calcined HZSM-5, or called “a hybrid catalyst”, was also tested in this work. The zinc oxide precursor was co-precipitated with alumina in order to form a ZnO-Al₂O₃ co-catalyst prior to incorporation with the calcined HZSM-5 by physical mixing method, according to the details described in Chapter 3. The effect of hybrid catalyst on aromatic production is explained as follows.

The ethanol conversion and product distribution are reported in Table 4.4. It is found that the bioethanol conversions obtained both zinc oxide-promoted HZSM-5 and hybrid catalysts are slightly lower than that of HZSM-5; however, it is an insignificant change. On the other hand, both oil yield and aromatic content from the hybrid catalyst are higher than those of ZnO-containing HZSM-5 and pure HZSM-5. As observed, the oil production is markedly improved by approximately 70 % as compared to that of HZSM-5 and about 35 % as compared to that of ZnO-containing HZSM-5. In terms of aromatic production, it can be noticed that the aromatization activity of zinc oxide-supported HZSM-5 is still low, whereas the catalytic activity of the hybrid catalyst toward aromatic formation is significantly higher. In terms of gaseous product, the gas yields obtained from ZHZ5 and Z+HZ5

are slightly lower than that of the pure HZSM-5. A significant amount of carbon dioxide is generated over the ZHZ5 and Z+HZ5. The ethane and mixed C3 are still major components in the gaseous product.

Table 4.4 Product distribution over the hybrid catalyst in the single-bed systems

	HZ5	ZHZ5	Z+HZ5
Ethanol Conversion (%)	85.0	82.8	79.9
Product yield (%)			
Total gas	56.2	53.7	49.5
Total oil	10.3	13.2	17.8
Total aromatics in oil	9.1	12.7	17.1
Gas Composition (%)			
Methane	10.1	8.9	8.3
Ethylene	7.6	5.8	5.9
Ethane	20.8	21.5	17.8
C3	40.9	12.5	15.4
C4	4.5	3.0	1.4
C5+	2.4	3.6	2.2
CO ₂	13.6	44.8	48.9
	100.0	100.0	100.0
Oil Composition (%)			
Monoaromatics	87.0	88.5	87.1
Diaromatics	1.3	7.9	9.3
Triaromatics	< 0.1	< 0.1	< 0.1
Non-aromatics	11.7	3.6	3.6
	100.0	100.0	100.0

Data were taken at the fifth hour of time-on-stream

The increase of aromatic production over the hybrid catalyst may be resulted from the synergy between ZnO-Al₂O₃ co-precipitate and HZSM-5 catalyst. As proposed by a few authors, the increased performance of a hybrid catalyst can be explained by the “sink” action of ZnO-Al₂O₃ co-catalyst involving hydrogen back-spillover or hydrogen reverse-spillover phenomena (Dufresne and Le Van Mao, 1994). Namely, some hydrogen produced over the zeolite’ surface by several acid catalysis reactions can migrate to ZnO-Al₂O₃ co-catalyst phase and then adsorb with

that surface. These migrating hydrogen species, which is denoted as spillover hydrogen species, are further desorbed as a molecular hydrogen gas. In the other word, the presence of co-catalyst can help to increase the removal of spillover hydrogen species that might exist in the HZSM-5 zeolite channel or surface to the co-catalyst's surface. This increases the aromatization occurring over the zeolite acid sites as well as help to reduce the reverse of aromatics to cycloalkane and/or cycloalkene.

4.3 Influence of Dual-Bed Catalytic Systems

In a dual bed system, bioethanol is converted to ethylene as a main product by using $\text{MgHPO}_4/\text{Al}_2\text{O}_3$ in Bed #1. Then, the ethylene is passed to Bed #2 to convert to liquid hydrocarbons by using several HZSM-5-based catalysts. The $\text{MgHPO}_4/\text{Al}_2\text{O}_3$ catalyst was the only catalyst used in the first bed, whereas several catalysts were employed in the second bed. Thus, the catalytic activity of $\text{MgHPO}_4/\text{Al}_2\text{O}_3$ is first examined, and the results are discussed in Section 4.3.1, and then used to explain the activity of dual bed systems of catalysts, which is discussed in Section 4.3.2. The reaction temperature at the first and second beds was controlled at 370 °C and 500 °C, respectively.

4.3.1 Catalytic Performance of $\text{MgHPO}_4/\text{Al}_2\text{O}_3$ on Ethylene Formation

To be able to explain the results of the dual bed cases, the catalytic activity of MgHPO_4 -added alumina in the catalytic Bed #1 for ethylene production needs to be known. The activity test was performed in the absence of any other catalyst packed in the second bed. The results are presented in Figure 4.1. At the beginning, ethylene selectivity reaches 100 %, but it drops to 80 % since the other products such as C3 – C5 hydrocarbons are later formed. Maximum 83 % bioethanol is converted to several hydrocarbon products consisting of mainly ethylene and some amount of light alkene and alkane such as ethane, propane, propylene, mixed C4, and mixed C5. About more than 80 % ethylene selectivity is obtained quite steadily along five hours of time-on stream. Approximately, 10 – 15 % selectivity of C5 hydrocarbons is co-produced, and the others are together formed at less than 5 %

selectivity. No liquid product is produced using the MgHPO_4 -doped alumina catalyst. Consequently, it can be suggested that the 0.5 wt% MgHPO_4 -added alumina catalyst can practically maintain its activity both on bioethanol conversion and ethylene selectivity in a long period of time. Moreover, its ethylene-rich effluent was then directly passed, as an ethylene-rich feed, to the catalytic Bed #2 to further convert to heavy hydrocarbons like aromatics. Therefore, 0.5 wt% MgHPO_4 -doped Al_2O_3 is hereby called as an “ethylene producing catalyst”.

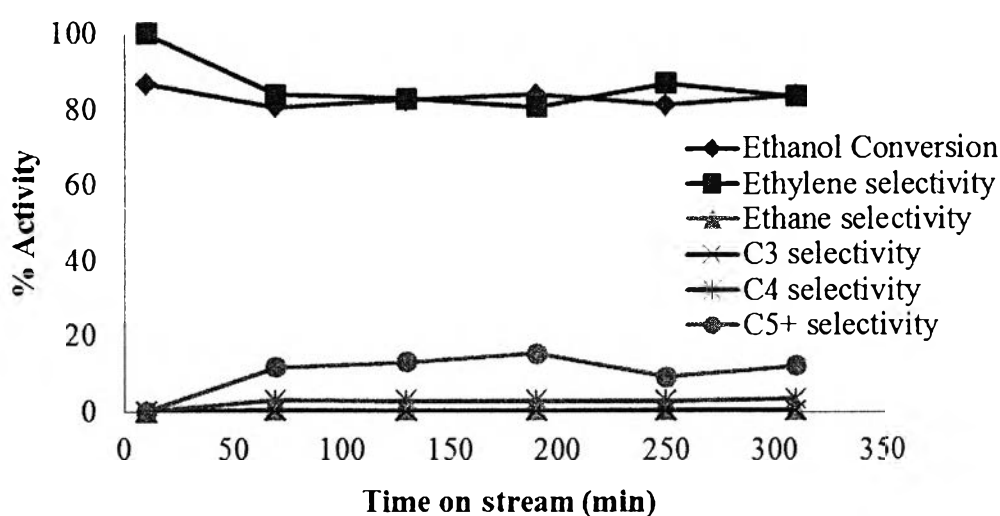


Figure 4.1 Bioethanol conversion and product selectivity over the catalytic Bed #1 of 0.5 wt% MgHPO_4 -added alumina.

4.3.2 Activity of Dual-Bed Catalytic Systems

In this part, the ethylene producing catalyst, 0.5 wt% $\text{MgHPO}_4/\text{Al}_2\text{O}_3$, was packed on the first catalytic bed, whereas the catalysts used in the second bed were pure HZSM-5, $\text{Ga}_2\text{O}_3/\text{HZSM-5}$, $\text{ZnO}/\text{HZSM-5}$, and $\text{ZnO-Al}_2\text{O}_3$ combined with HZSM-5 (Hybrid catalyst). It is noted here that these catalysts have already been tested for their own activity in the single-bed catalytic system in Parts 4.2.1 and 4.2.2. Using the dual-bed catalytic system, the total ethanol conversion and product distribution are reported in Table 4.5. The total ethanol conversion is found at 88.5 % maximum using the hybrid catalyst, whereas that of the other catalysts achieves about 83-85 % conversion. These results can be implied that the total bioethanol

conversion obtained from the two-bed systems is slightly improved from the one from the single bed of $\text{MgHPO}_4/\text{Al}_2\text{O}_3$.

Table 4.5 Product distribution from using dual-bed catalytic systems

	EPC:HZ5	EPC:GHZ5	EPC:ZHZ5	EPC:Z+HZ5
Ethanol Conversion (%)	83.7	85.6	85.3	88.5
Product Yield (%)				
Total gas	50.6	43.5	53.8	45.0
Total oil	16.1	23.0	12.7	21.1
Total aromatics in oil	15.5	22.1	12.3	20.3
Gas Composition (%)				
Methane	7.6	9.4	12.9	10.0
Ethylene	6.2	5.4	2.3	13.1
Ethane	21.1	21.1	26.5	23.4
C3	52.0	50.7	9.7	4.3
C4	6.4	3.0	1.6	3.3
C5+	3.0	4.2	2.5	7.5
CO ₂	3.7	6.2	44.5	38.4
	100.0	100.0	100.0	100.0
Oil composition (%)				
Monoaromatics	85.1	84.0	87.8	90.3
Diaromatics	11.4	12.3	8.4	6.0
Triaromatics	< 0.1	< 0.1	< 0.1	< 0.1
Non-aromatics	3.5	3.7	3.8	3.7
	100.0	100.0	100.0	100.0

Data were taken at the fifth hour of time-on-stream

Note: Catalyst packed at 1st bed

- EPC = Ethylene producing catalyst (0.5 wt% $\text{MgHPO}_4/\text{Al}_2\text{O}_3$)

Catalysts packed at 2nd bed

- HZ5 = HZSM-5
- GHZ5 = $\text{Ga}_2\text{O}_3/\text{HZSM-5}$
- ZHZ5 = $\text{ZnO}/\text{HZSM-5}$
- Z+HZ5 = $\text{ZnO-Al}_2\text{O}_3$ combined with HZSM-5 (hybrid catalyst)

The product yield obtained from the dual-bed catalytic systems is also presented in Table 4.5. It is found that the oil yield is decreased in the order: EPC:GHZ5 > EPC:HZ5 > EPC:ZHZ5 > EPC:Z+HZ5. Moreover, it is noticed that Ga₂O₃/HZSM-5 used in the second bed gives the highest oil yield with the highest mono-aromatic content. Figure 4.2 (a) and (b) demonstrate the comparison between product yields obtained from the single-bed catalytic systems and dual-bed catalytic systems. The comparison between case by case reveals that the total oil yields obtained from the dual-bed systems are dramatically higher than those from the single-bed systems, except the case of EPC:ZHZ5. The production of oil can be enhanced by 56 %, 26 %, and 19 % from those produced by HZ5, GHZ5, and Z+HZ5, respectively. In addition, it can be observed that the oils mainly contain at least 96.2 wt% aromatic hydrocarbons for all cases. Moreover, the case of EPC:GHZ5 also gives the highest oil yield and aromatic yield.

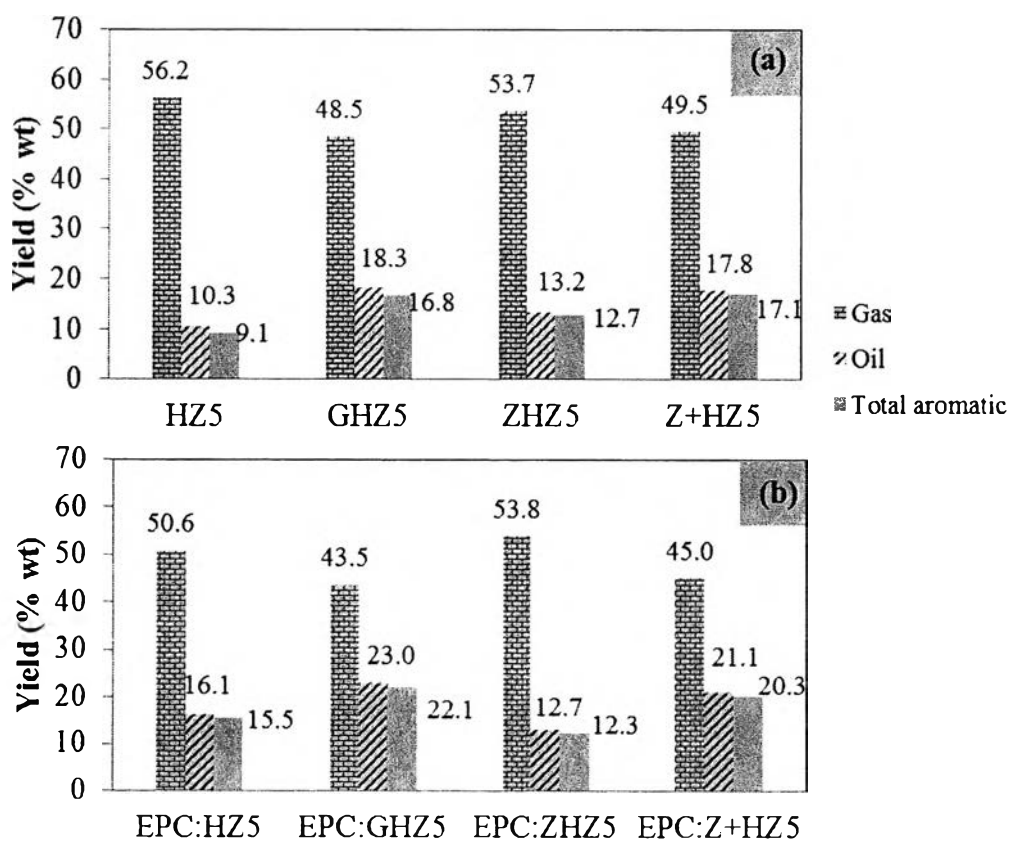


Figure 4.2 Comparison of product yields obtained from (a) single-bed catalytic systems, and (b) dual-bed catalytic systems.

According to the results, it can be noted that the ability of aromatic formation in the dual-bed catalytic systems is better than the single-bed catalytic systems. After ethanol is converted to ethylene at the first catalytic bed, the ethylene-rich feed is continuously fed into the second bed. From the previous report, it was discovered that ethylene was more active as a reactant for oligomerization, isomerization, cracking, cyclization, hydrogen transfer, dehydrogenation, and dehydrocyclization than ethanol (Brathos *et al.*, 2006). Therefore, the use of ethanol as a direct feed in the single bed system takes a higher number of acid sites of zeolite, contributing for the ethanol dehydration. On contrary, with using ethylene-rich feed, ethylene can be activated immediately by all available acid sites of catalyst. Possibly, the shorter reaction pathway in the dual-bed catalytic systems causes more effective aromatic formation than using the single-bed systems.

Table 4.6 Aromatic production from dual-bed catalytic systems

Component	Composition (wt%)			
	EPC:HZ5	EPC:GHZ5	EPC:ZHZ5	EPC:Z+HZ5
Non-aromatics	3.53	3.68	3.79	3.74
Benzene	20.45	19.92	21.31	23.51
Toluene	41.05	42.06	43.24	44.99
<i>p</i> -Xylene	4.36	4.46	4.92	4.57
<i>m</i> -Xylene	9.55	10.01	10.8	9.91
<i>o</i> -Xylene	4.51	4.67	4.97	4.57
Ethylbenzene	1.92	0.93	0.85	1.10
C9	3.22	1.92	1.70	1.65
C10+	11.42	12.34	8.42	5.95
BTX/total aromatic fraction	0.83	0.84	0.89	0.92

Table 4.6 exhibits the qualitative analysis of oil obtained from the EPC:HZ5, EPC:GHZ5, EPC:ZHZ5, and EPC:Z+HZ5 cases, which the last case gives the best results of BTX selectivity. Moreover, the obtained oil mainly consists of aromatics, especially mono-aromatics. About 92 wt% of BTX in total aromatic components is observed whereas the concentration of *p*-xylene is about 24 % of mixed xylenes.

The oils obtained from the sing-bed and dual-bed catalytic systems were cut into petroleum fractions, according to true boiling point obtained from SIMDIST-GC analysis, as exhibited in Table 4.7.

Table 4.7 Boiling point range of petroleum fractions (Dũng *et al.*, 2009)

Fraction	Boiling point (°C)
Gasoline	< 149
Kerosene	149-232
Gas oil	232-343
Light vacuum gas oil	343-371
Heavy vacuum gas oil	> 371

Figure 4.3 (a) and (b) shows the petroleum fractions obtained from using the single-bed catalytic systems and the dual-bed catalytic systems, respectively. The derived oils from all catalysts are mainly distributed in the range of gasoline. The dopants (Ga_2O_3 and ZnO) on the HZSM-5 and the hybrid catalyst cause a slight increase of gasoline with a subsequent decrease in kerosene fraction. It means that the addition of some dopants into the HZSM-5 catalyst can slightly improve the catalytic cracking activity on which heavier hydrocarbons are cracked into lighter hydrocarbons. Moreover, the result in Figure 4.3 (b) shows the same trend as using the single-bed catalytic systems. However, the gasoline fraction is also slightly higher with using the dual-bed catalytic systems.

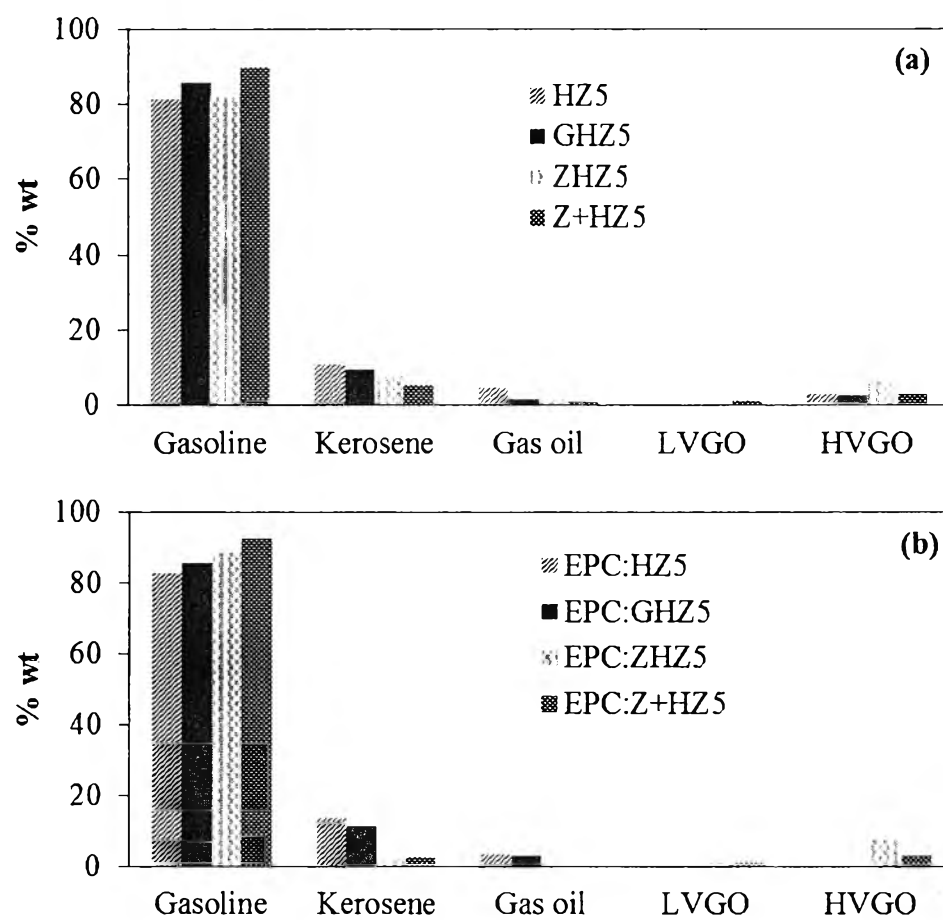


Figure 4.3 Petroleum fractions in oils obtained from using (a) the single-bed catalytic systems, and (b) the dual-bed catalytic systems.

4.4 Plant Design for Economic Pre-feasibility Study

To start the economic pre-feasibility evaluation, an overview of process layout is firstly discussed for further estimation. The ethanol-based aromatic manufacturing plant in this study was preliminarily designed. The design of process involving the bio-ethanol conversion to aromatic hydrocarbons was carried out under the concept of using a series of two reactors where the ethanol dehydration and ethylene aromatization reactions take place in series.

The essential parameters for the process plant design are shown in Table 4.8. Moreover, overall of basic assumptions, scope, and limitations of this work are also clearly identified as listed below:

- The highest yield oil from the experiment in the previous section, which is obtained from the two consecutive beds of $\text{MgHPO}_4/\text{Al}_2\text{O}_3$ and $\text{Ga}_2\text{O}_3/\text{HZSM-5}$, is used as the basis for plant design and pre-feasibility study.
- The bio-ethanol used as a feedstock for aromatic production in the designed process is supplied by Sapthip Company Limited. Its concentration is fixed at 99.5 % ethanol in the feed.
- The gaseous product is sold as natural gas according to its heating value, and the aromatic-containing oil product is sold as naphtha.
- The liquid storage tank is installed on-site to storage the produced oil hydrocarbons prior to transport to customer.
- Raw materials, gas and oil products are transported via truck or pipe.
- ISBL and OSBL are included in the economic pre-feasibility evaluation.
- Electricity is purchased from Province Electricity Authority.
- Steam and coolants used in the designed plant are purchased outside sources.
- Waste water treatment unit is included in this designed process plant.

Table 4.8 Summary of the bioethanol-based aromatic plant design parameters

Parameter	Assigned value
Plant Capacity (based on bio-ethanol)	54,700 tons per year
Bioethanol feed purity	99.5 vol % Ethanol
Bioethanol feed rate	172.2 tons per day
Bioethanol conversion	85.6 %
Number of working days	8,000 hours per year (about 333 days)
Yield of oil products	11,300 tons per year
Yield of aromatics in oil	10,882 tons per year
Spec. of desired product	96.3 wt % aromatics in oil
Yield of natural gas	21,356 tons per year
Operation Mode	Continuous (24 hours)

The block diagram of the designed process as illustrated in Figure 4.4 is primarily present to understand the overview of process for aromatic production from bioethanol using the two consecutive reactors. Ten important units are shown in this process: (1) Ethanol vaporizer, (2) Furnace, (3) Reactor Unit #1, (4) Reactor Unit #2, (5) Waste Heat Boiler, (6) Vapor-Liquid Separator, (7) Compressor, and (8) Liquid-Liquid Phase Separator.

4.4.1 Process Description

The process flow diagram (PFD) for aromatic production from bio-ethanol is shown in Figure 4.5. The process basically consists of two main plants. One is a series of reactor unit illustrating in the A-100 region, and another is the product separation plants illustrating in the A-200 region. The former is the area involving the overall reaction of bio-ethanol aromatization which starts with ethanol dehydration to ethylene and then ethylene aromatization. The latter is the region where the necessary units of the product separation are operated.

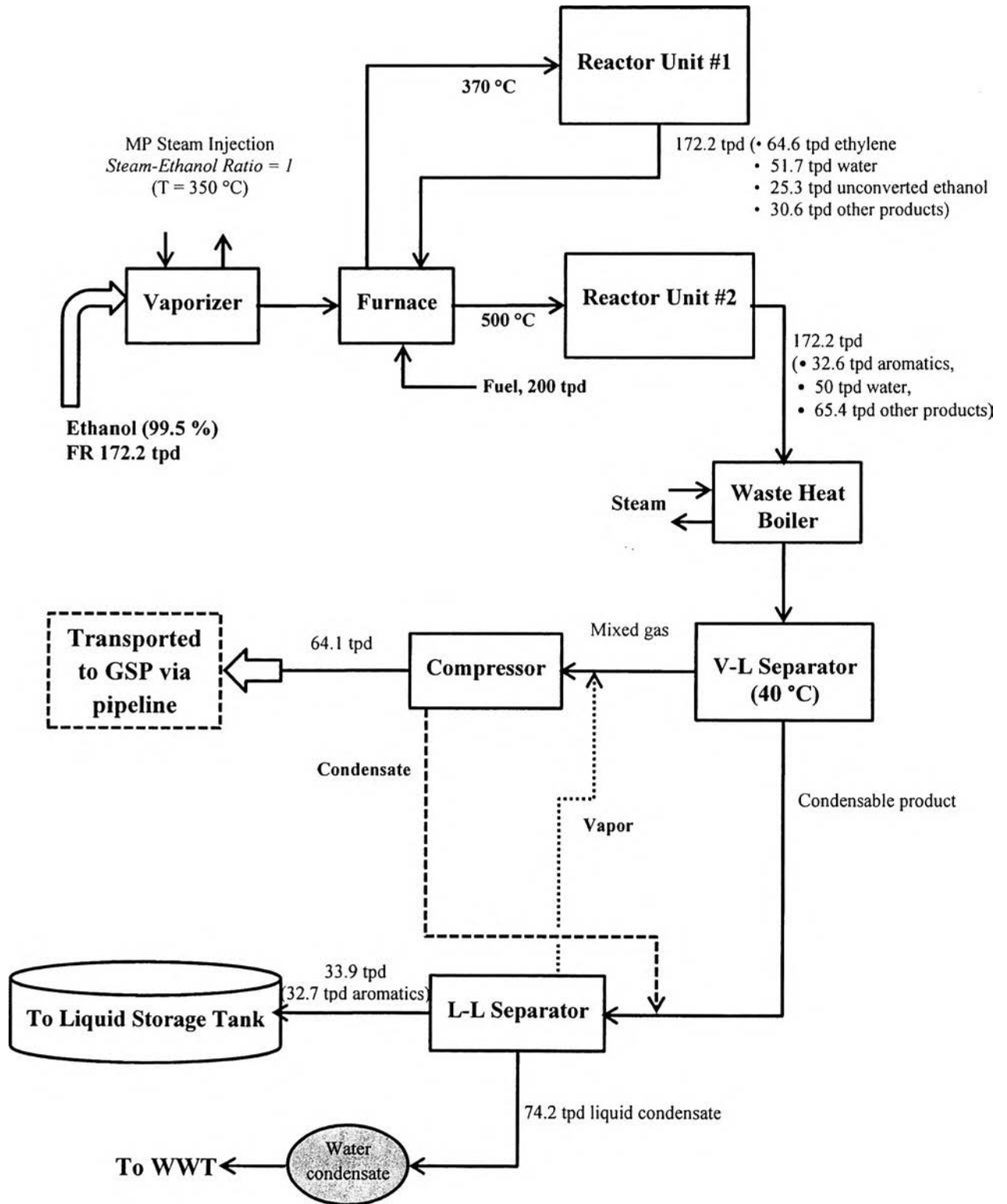


Figure 4.4 Block diagram of process configuration for ethanol-based aromatic production plant.

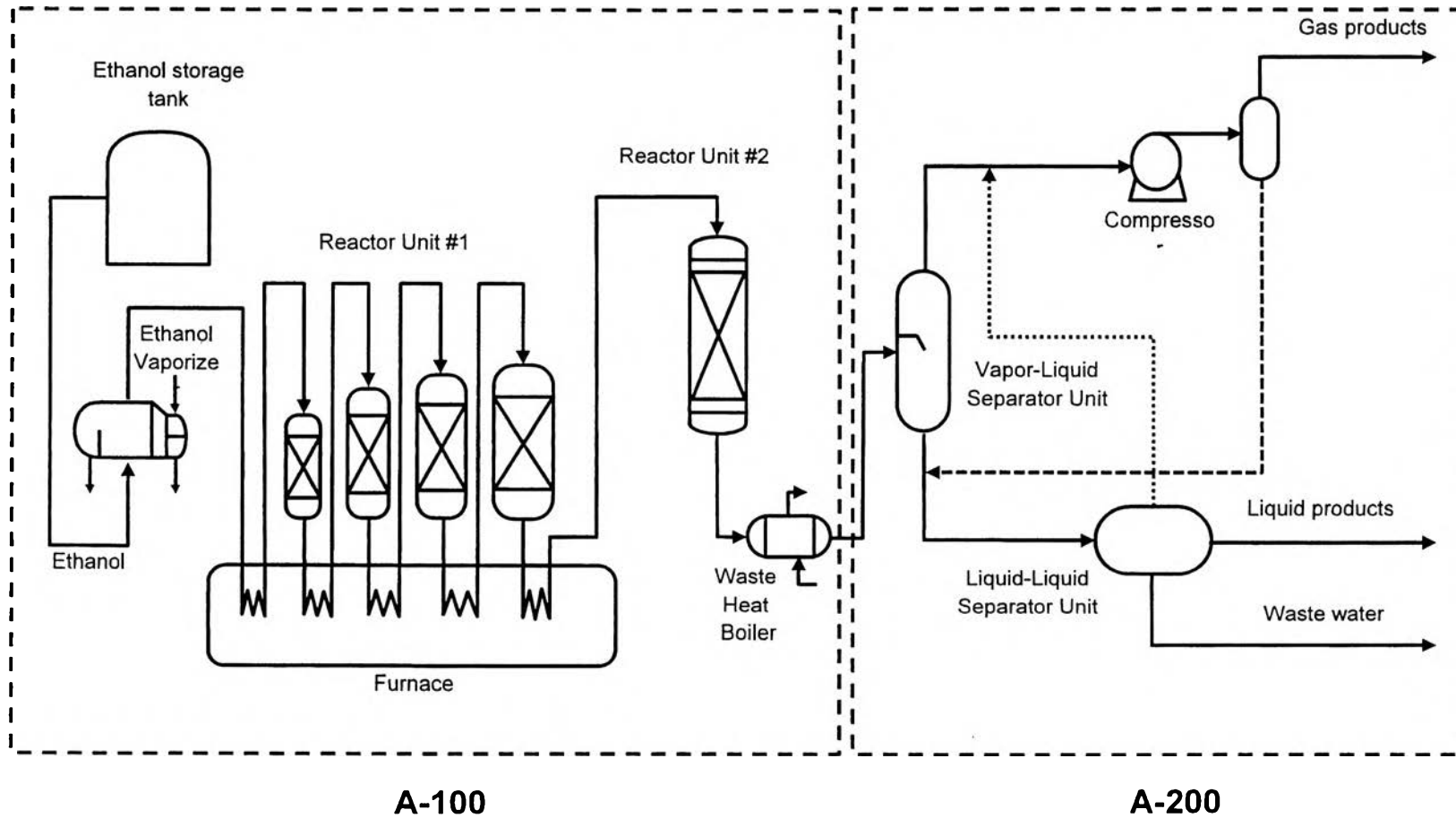


Figure 4.5 Process flow diagram of the bioethanol-based aromatic production plant.

To begin the operation, 172.2 tons per day of 99.5 vol% bio-ethanol is fed from the storage tank to an ethanol vaporizer. The superheated steam with medium pressure (10.4 bar) is performed in vaporization, to vaporize the bio-ethanol from liquid phase to vapor phase. Subsequently, the vaporized bio-ethanol is pre-heated to 370 °C in a furnace, and next fed into the Reactor Unit #1 consisting of the four catalytic beds with the 0.5 wt% magnesium hydrophosphate-doped alumina catalyst (0.5 % wt $\text{MgHPO}_4/\text{Al}_2\text{O}_3$) packed in each bed. Bio-ethanol is converted to ethylene as it passes over the catalyst, and about 30 % ethanol conversion is achieved from the first catalytic bed. The partially converted gas coming out the first bed is reheated in the furnace, and then passed through the second catalytic bed. Likewise, the cycles at the third and fourth catalytic beds are operated in the same way as the first two beds. The ethanol conversion is increased to 85.6 % after leaving the last catalytic bed.

The outstream product obtained from the Reactor Unit #1 approximately contains 37.5 wt% ethylene yield, and not only the ethylene is generated, but also some by-products can be produced during the ethanol dehydration such as methane, ethane, propylene, propane, butylene, and carbon dioxide. Further, the effluent gas leaving from the last bed of the Reactor Unit #1 is passed to the Reactor Unit #2, and its temperature is heated to 500 °C to enable the ethylene aromatization in the Reactor Unit #2, which contains the gallium oxide-supported HZSM-5 catalyst. About 94.6 % of the ethylene is converted to the heavier hydrocarbons including aromatics compound predominantly. After leaving the Reactor Unit #2, the hot reactor effluent is delivered to a waste heat boiler, in order to recover some heat to the process steam. Subsequently, the effluent is passed to a flash drum (vapor-liquid separator), where the gaseous products are separated on the top of the vessel, while the condensate is settle to the bottom of the vessel.

Next, the condensate is fed into a liquid-liquid phase separator in order to separate liquid hydrocarbons from water. The water is removed to a waste water treatment process, whereas the liquid hydrocarbons are sent to the liquid storage tank. Unfortunately, it still has some components (i.e. lighter hydrocarbons, unreacted bio-ethanol, aldehyde etc.) in the liquid phase that can be vaporized to the vapor phase. Consequently, these gaseous components are further sent to a

compressor. Simultaneously, the overhead leaving from the vapor-liquid separator is also passed to the same compressor connected with intercooler knockout drum. It means that the remaining condensate (water-liquid hydrocarbons mixture) in the gas phase is dropped in a knockout drum, and then sent back to the liquid-liquid phase separator. The remaining gas is ultimately transferred to the gas separation plant via pipeline system. From above process, about 33.9 tons per day of the liquid hydrocarbons containing 96.3 wt% aromatics are produced, and about 64.1 tons per day of gaseous products, whose component similar to natural gas, are generated.

4.4.2 Description of Each Unit

According to the description of process, each unit is described in more details in the section. Figures 4.6 and 4.7 illustrate the process flow diagram of reaction system and the process flow diagram of product separation plant, respectively. The function of each unit, their operating conditions, as well as utilities is discussed in details as follows:

4.4.2.1 Reaction System (A-100 Region)

a) Bio-ethanol Storage Tank

A commercial grade bio-ethanol at the concentration of 99.5 % is used as the raw material in this process. The bio-ethanol is stored in a storage tank with the 450,000 gallon maximum capacity (13,400 metric tons of ethanol at 25 °C).

b) Vaporizer (E-111)

The vaporization process is required before the bio-ethanol enters to the reactor. The bio-ethanol supplied from storage tank is pumped into a kettle-type vaporizer (E-111) at the feed rate of 7.2 metric tons per hour. The medium pressure steam (10.4 bar) is performed to vaporize the bio-ethanol feed, and the temperature is ultimately raised to 135 °C.

c) Furnace (Q-112)

After the bio-ethanol has been vaporized, the bio-ethanol vapor is next passed to a furnace (Q-112) in order to raise its temperature to 370 °C, which is the desired reaction temperature. The superheated bio-ethanol is further fed to the Reactor Unit #1 (R-120). Besides preheating the bio-ethanol vapor, the furnace (Q-112) also reheats the effluent gas from each catalytic bed in the Reactor Unit #1 (R-120).

d) Reactor Unit #1 (R-120)

The reactor Unit #1 (R-120) is the most important unit in the bio-ethanol dehydration to ethylene process. It is where the conversion of bio-ethanol to ethylene takes place. The reactor is a multi-bed adiabatic reactor consisting of four catalytic beds with the Syndol catalyst or alumina oxide-based catalyst. The reaction is operated at 370 °C and under the pressure of 1.0 bar. At the first catalytic bed (R-121), only 30 % of bio-ethanol is converted. Because of the bio-ethanol dehydration to ethylene is a catalytic endothermic reaction, which causes a reaction temperature drop. Therefore, it is necessary to reheat the effluent gases to the reaction temperature (370 °C) before passing it to the next following bed in order to raise the reaction rate and bio-ethanol conversion. Similarly, the reaction/reheat cycles are conducted in the second (R-122), the third (R-123), and the fourth catalytic bed (R-124) where more bio-ethanol is converted. From the process above, the bio-ethanol conversion is progressively increased to 85.6 %. It means that about 64.8 tons per day of ethylene can be produced. However, some by products can be co-produced such as methane, ethane, propylene, propane, carbon dioxide, and hydrogen.

e) Reactor Unit #2 (R-132)

After the reaction in the Reactor Unit #1 (R-120), the outstream product leaving from the last bed (R-124) is used as the incoming feedstock for the Reactor Unit #2 (R-132). Prior to entering to the second reactor, the gas is heated in the furnace (Q-112) to raise the temperature to 500 °C to enable the ethylene aromatization. However, the reactor Unit #2 (R-132) is the most important unit in the ethylene aromatization process. It is where the conversion of ethylene to aromatic hydrocarbons occurs. The reactor is designed to be a single-bed adiabatic

reactor with a modified HZSM-5 zeolite catalyst bed. About 94.6 % of the ethylene obtained from the Reactor Unit #1 (R-120) is converted. The total outstreams leaving the Reactor Unit #2 (R-132) contains 19.7 wt % oil yield. Next, the hot reactor effluent is passed to the product separation plant. Nevertheless, the obtained product is mostly consisted of aromatic hydrocarbons.

f) Waste Heat Boiler (E-133)

Before the hot effluent leaving from the Reactor Unit #2 (R-132) is then sent to the product separation process (A-200 region), it is passed to a waste heat boiler (E-133) in order to recover some heat to produce a process steam. The effluent is cooled to 90 °C. Finally, the medium pressure steam is produced by the hot gases, and used in the plant.

4.4.2.2 Product separation plant (A-200 Region)

a) Vapor-Liquid Separator : Knockout Drum (F-221)

In a vapor-liquid knockout drum (F-221), it has been used for the purpose in the separation of heavy hydrocarbons containing aromatics from lighter hydrocarbons. The cooled vapor is fed to a vessel, and additionally cooled down to 40 °C. The liquid product is condensed to the bottom of the vessel, and is withdrawn. The vapor is exited on the top and next transferred to a compressor unit, C-120. At least about 63 tons per day of liquid is dropped, which includes both liquid hydrocarbons and water condensate. The overhead is mainly comprised of the lighter hydrocarbons similar to a natural gas.

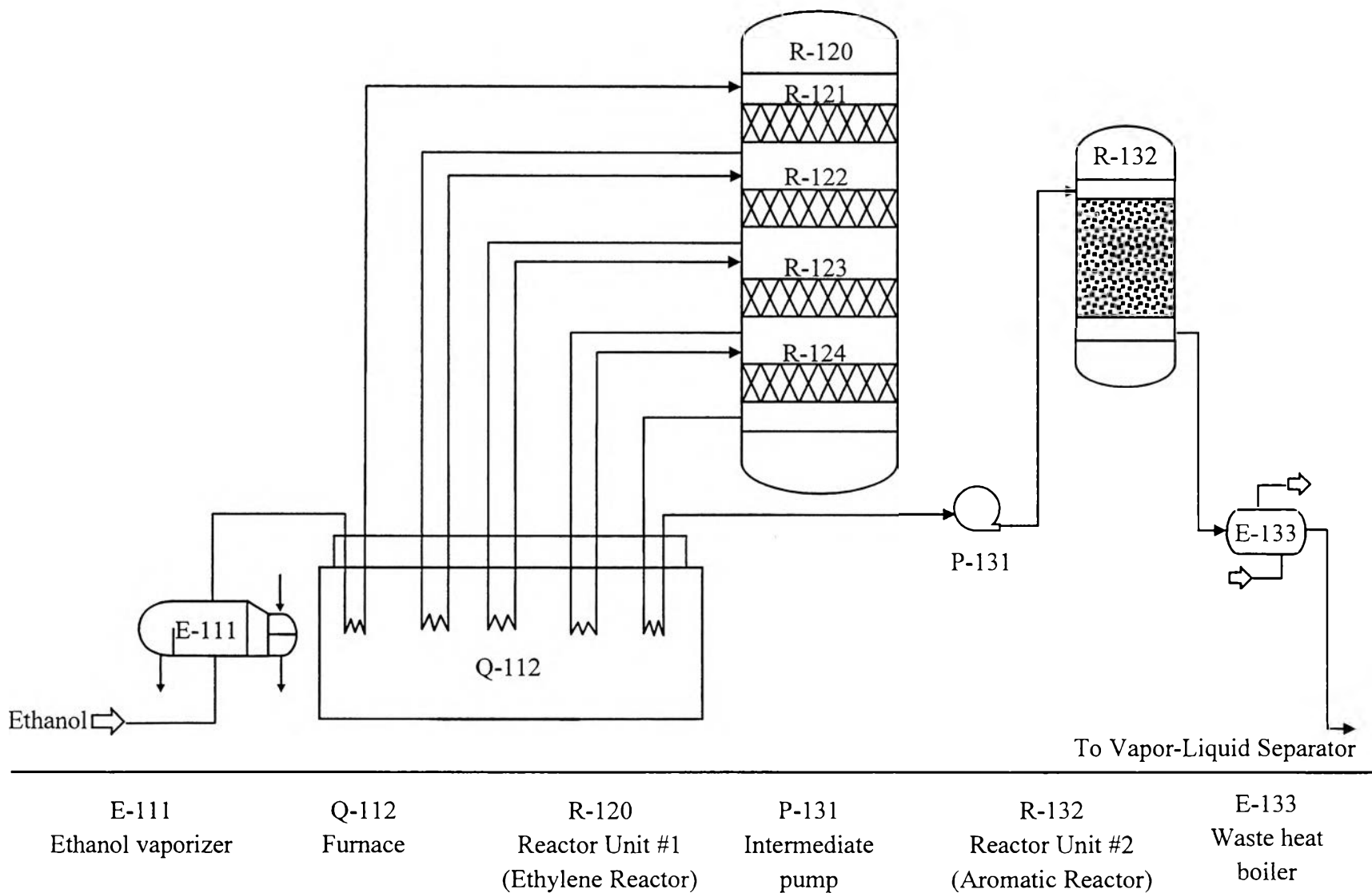


Figure 4.6 Process flow diagram of reaction system (A-100 Region).

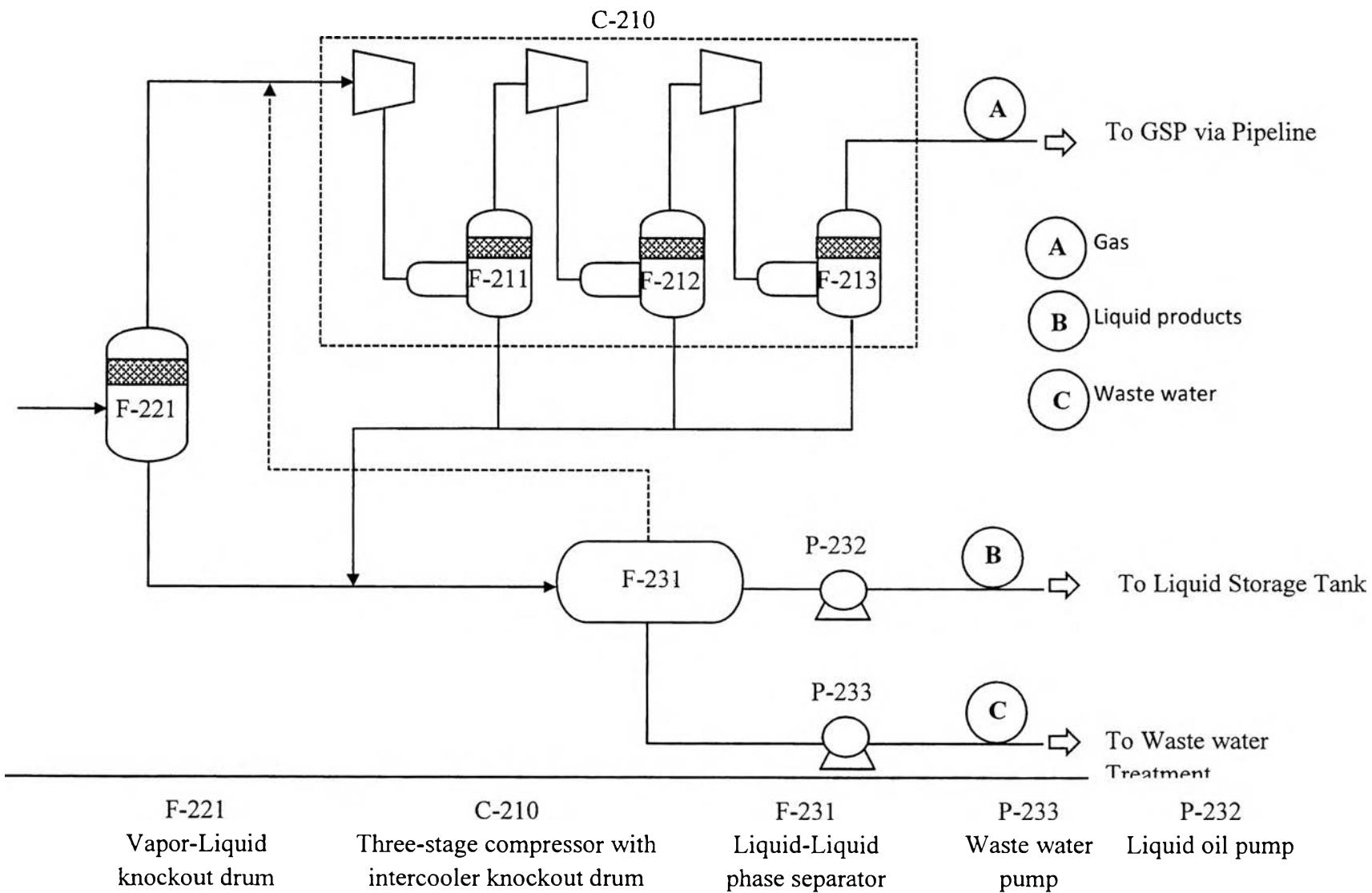


Figure 4.7 Process flow diagram of product separation plant (A-200 Region).

b) Vapor-Liquid Separator : Knockout Drum (F-221)

In a vapor-liquid knockout drum (F-221), it has been used for the purpose in the separation of heavy hydrocarbons containing aromatics from lighter hydrocarbons. The cooled vapor is fed to a vessel, and additionally cooled down to 40 °C. The liquid product is condensed to the bottom of the vessel, and is withdrawn. The vapor is exited on the top and next transferred to a compressor unit, C-120. At least about 63 tons per day of liquid is dropped, which includes both liquid hydrocarbons and water condensate. The overhead is mainly comprised of the lighter hydrocarbons similar to a natural gas.

c) Compressor (C-210)

For the compressor unit (C-120), the three-stage compressors are used to increase the overhead pressure to 27 bar. The pressure ratio of 3 is performed in each step. The intercooler connected knock-out drums (F-211, F-212, and F-213) are installed between compressors in order to cool the compressed gas to 38 °C. The entrained condensate is subsequently condensed in knockout drums (F-211, F-212, and F-213), and then sent to a liquid-liquid phase separator (F-231). Finally, the compressed gas is sent to a customer (such as a gas separation plant) via pipeline. About 64 tons of the total gas products are produced in each day.

d) Liquid-Liquid Phase Separator (F-231)

Since the condensate from the vapor-liquid separator (F-221) mainly consists of the liquid hydrocarbons and water, in order to separate the liquid hydrocarbons from water, the condensate is fed into the liquid-liquid phase separator (F-231). The separation is based on the specific gravity difference between the liquid hydrocarbon and the water. The water is fallen to the bottom of a unit and removed as waste water for further treatment whereas the liquid hydrocarbons are separated on the top, and it is skimmed off and subsequently sent to store in an available storage tank. The gas that may occur in this step is sent to the compressor unit (C-120), and collected together with the gas product stream.

4.5 Economic Assessment and Pre-feasibility

The pre-feasibility evaluation for the aromatic manufacturing from bioethanol using two consecutive reactors system has been established based on material balance, according to the experimental data and several assumptions both from the catalyst testing and preliminary plant design in previous section. The yield obtained from two consecutive bed of $\text{MgHPO}_4/\text{Al}_2\text{O}_3$ and $\text{Ga}_2\text{O}_3/\text{HZSM-5}$ is employed for the designed aromatic-rich oil production plant. Additionally, the economic estimation is based on the ethanol consumption of 172.2 ton per day. The other necessary assumptions for economic pre-feasibility evaluation are exhibited in Table 4.9.

Regarding to the economic pre-feasibility, the complete cost estimation of this plant is included into three main sections, which are the total capital investment cost, the annual operating cost, and the annual revenue. A detailed breakdown of each part is provided in the next sections.

Table 4.9 Basis assumptions of the economic evaluation for naphtha production plant

Item	Unit	Value	Remark
Capacity	ton per year	10,882	Aromatic capacity
Working day	day per year	333	8,000 hour
Operating shift	shift	2	Including operator, foreman, and sale
OSBL: Steam & Cooling water		Available	
Raw material : Bio-ethanol 99.5%	Baht/Liter	17.2	Based on ethanol price from Thailoil company
Gaseous products	Baht/MilBTU	442.3	Natural gas price, 2012
Oil products	Baht/ton	25,600	Naphtha price, 2012
Depreciation	year	20	Economic life is 20 years
Waive income tax	%	30	All Capex is paid at zero year

4.5.1 Total Capital Investment Cost ($\pm 50\%$)

The total capital investment cost of aromatic-rich oil production plant is estimated based on the scope and limitations as described in Sections 4.4.1 and 4.4.2. The estimation of cost is based on the indexing method using the relationship of $Cost \propto Size^{0.6}$ which is scaled down from the real production plant as details shown in Appendix E (Figure E1 - E5). The total capital investment of this project is US\$ 75.74 millions or 2,272.2 millions Baht. This capital cost was adapted from the commercial ethylene production plant price of Chematur.

4.5.2 Annual Operating Cost Estimation

Typically, the estimate of operating costs can be divided into two main parts. The costs involving labor and maintenance work are the fixed operating costs, whereas the cost of raw material and utility is the variable operating costs. The details are summarized in Table 4.10. Moreover, the estimated value is also assumed to be equal in every years of all economic life (20 years). Figure 4.8 shows the distribution of operating costs. Around 86 % of total annual operating cost is contributed from raw material cost. It means that the raw material cost is an important parameter that affects to the total investment cost.

Table 4.10 Annual operating cost of naphtha production plant

Items	Millions Baht per year
Raw material cost	1,249.7
Labor and maintenance cost	70.4
Utilities cost	138.8
Total operating cost	1,458.9

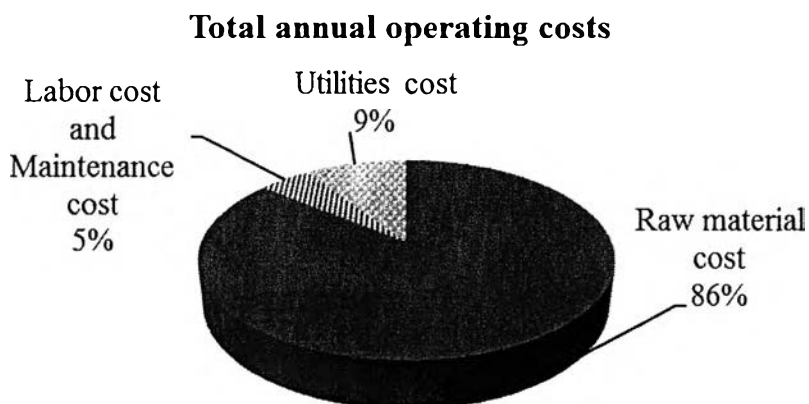


Figure 4.8 Operating cost distribution.

4.5.3 Annual Revenue Estimation

The revenues of the plant mainly come from the selling of both gaseous products and liquid products. Based on the product composition, the gaseous product mainly consists of C1 – C4 hydrocarbons; thus, it is sold as a natural gas to gas separation plant according to its heating value, whereas the liquid product is in the naphtha range hydrocarbons, mainly contains aromatic hydrocarbons. Therefore, it is sold as a naphtha product. The annual revenue of each product is concluded in Table 4.11. The details are also shown in Appendix E (Table E5 - E6). The total achieved revenue is 728.4 Millions Baht per year.

Table 4.11 Annual revenue of bioethanol-based naphtha production plant

Product	Capacity (tons/year)	Price	Annual revenue (Millions Baht)
Natural gas	21,356	442.3 (Baht/Mil.BTU)	439.1
Liquid hydrocarbon (Naphtha range)	11,300	25,600 (Baht/ton)	289.3

4.5.4 Economic Evaluation

The total capital investment cost, the annual operating costs, and the annual revenue in Sections 4.5.1 to 4.5.3 are employed to evaluate the economic pre-feasibility of naphtha production plant. The profitability indicators are internal rate of return (IRR), net present value (NPV), payback period (PB), and profitability index (PI). Moreover, the total annual profits can be calculated as the equation below. All details are shown in Appendix E (Table E3).

$$\text{Net annual profits} = \text{Net annual revenue} - \text{Net annual operating costs}$$

The values of profitability indicators are reported in Table 4.12. As a result, the higher annual operating cost than the total revenue causes the negative annual profit (margin). It also causes the negative net present value (NPV). The profitability index and payback period cannot be estimated. Since the annual profit is minus sign, the internal rate of return cannot be calculated. In summary, it can be inferred that the plant is not commercially feasible.

Table 4.12 Estimated economic indexes of naphtha production plant

Profitability indicator	Value	Unit
Annual profits	-730.6	Mil. Baht/year
IRR in tax	-	% per year
NPV after tax	-6,201.17	Mil. Baht
Profitability index (NPV/Fixed cost)	-	-
Simple payback period before tax	-	Months

4.5.5 Sensitivity Analysis

Since the project is not commercially possible, the sensitivity analysis is performed to find raw material price and product (both gas and oil) prices that make project feasible.

4.5.5.1 Ethanol Price

As presented in Section 4.5.2, the cost of raw material is likely to be a crucial variable that can affect to the economic pre-feasibility of the plant. Figure 4.9 exhibits the sensitivity of the internal rate of return and payback period toward the change of ethanol price. The decrease in ethanol price results in the increase in the internal rate of return and the decrease in payback period. When the ethanol price is reduced to 0.7 Baht/liter, 15 % of IRR is obtained. However, this ethanol price is not likely possible.

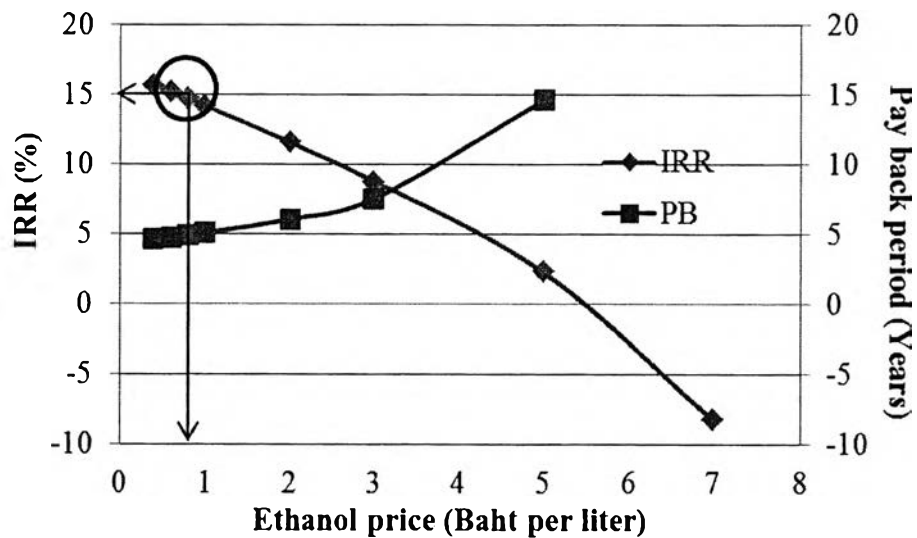


Figure 4.9 Sensitivity of internal rate of return and payback period toward ethanol price.

4.5.5.2 Product Prices (Both gas and oil)

The product prices are the other sensitive parameters that can affect to the economic pre-feasibility of the production plant. Figure 4.10 shows the sensitivity of the internal rate of return and payback period toward the change of gas and oil prices. The increasing product prices result in the increase in the internal rate of return and the decrease in payback period. When both product prices are approximately 165 % higher than the original prices, the 15 % of IRR is obtained.

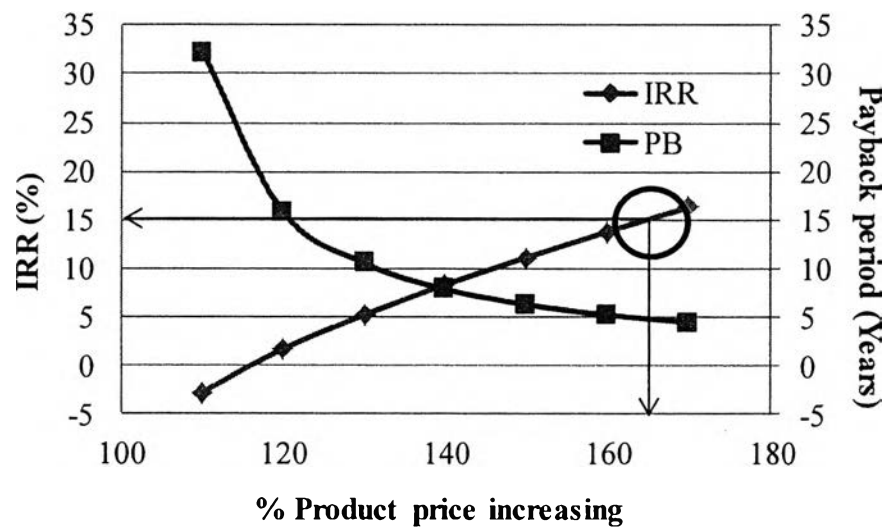


Figure 4.10 Sensitivity of internal rate of return and payback period toward the product price change of the oil production plant.